Instantaneous imaging of ozone in a gliding arc discharge using photofragmentation laser-induced fluorescence

Larsson, Kajsa; Hot, Dina; Gao, Jinlong; Kong, Chengdong; Li, Zhongshan; Aldén, Marcus; Bood, Joakim; Ehn, Andreas

Published in:
Journal of Physics D: Applied Physics

DOI:
10.1088/1361-6463/aab05b

2018

Document Version:
Publisher's PDF, also known as Version of record

Instantaneous imaging of ozone in a gliding arc discharge using photofragmentation laser-induced fluorescence

OPEN ACCESS
IOP Publishing
Journal of Physics D: Applied Physics
J. Phys. D: Appl. Phys. **51** (2018) 135203 (7pp)
https://doi.org/10.1088/1361-6463/aab05b

Instantaneous imaging of ozone in a gliding arc discharge using photofragmentation laser-induced fluorescence

Kajsa Larsson, Dina Hot, Jinlong Gao, Chengdong Kong, Zhongshan Li, Marcus Aldén, Joakim Bood and Andreas Ehn

Division of Combustion Physics, Lund University, Box 118, SE-221 00 Lund, Sweden

E-mail: joakim.bood@forbrf.lth.se

Received 10 November 2017, revised 9 February 2018
Accepted for publication 19 February 2018
Published 7 March 2018

Abstract

Ozone vapor, O_3, is here visualized in a gliding arc discharge using photofragmentation laser-induced fluorescence. Ozone is imaged by first photodissociating the O_3 molecule into an O radical and a vibrationally hot O_2 fragment by a pump photon. Thereafter, the vibrationally excited O_2 molecule absorbs a second (probe) photon that further transits the O_2-molecule to an excited electronic state, and hence, fluorescence from the deexcitation process in the molecule can be detected. Both the photodissociation and excitation processes are achieved within one 248 nm KrF excimer laser pulse that is formed into a laser sheet and the fluorescence is imaged using an intensified CCD camera. The laser-induced signal in the vicinity of the plasma column formed by the gliding arc is confirmed to stem from O_3 rather than plasma produced vibrationally hot O_2. While both these products can be produced in plasmas a second laser pulse at 266 nm was utilized to separate the pump- from the probe-processes. Such arrangement allowed lifetime studies of vibrationally hot O_2, which under these conditions were several orders of magnitude shorter than the lifetime of plasma-produced ozone.

Keywords: ozone, photofragmentation, laser-induced fluorescence, imaging, plasma, gliding arc

(Some figures may appear in colour only in the online journal)

Introduction

Plasma is used in various applications to, for example, increase the energy efficiency and enhance both the productivity and selectivity. Examples of such applications may be emission control of soot, UV generation, and CO_2 dissociation [1]. Plasma can be characterized into thermal and non-thermal plasma. In thermal plasma species such as neutral molecules and ions have the same temperature as free electrons, whereas in non-thermal plasmas the free electron temperature differs from the translational-, rotational-, vibrational-, and electronic temperature since the supplied electric energy is transferred to electrons increasing their temperature [2]. Non-thermal plasma has gained interest in the last couple of years due to its capacity to provide an environment with low gas- and high electron-temperature, thereby generating abundant reactive species. Non-thermal plasma may for example be formed by pulsed microwaves [3] or nanosecond high voltage pulses [4]. These types of plasma generation have shown promising results in combustion enhancement and combustion control [5–7]. Lee *et al* [2] built a rotating gliding arc setup to better understand plasma chemistry. For instance, they found that in their non-thermal rotating gliding arc setup the number of reactive species was increased, thereby enhancing the combustion efficiency, by increasing the arc length. Furthermore, the need for reducing pollution and increasing combustion

efficiency in order to comply with legislation and fulfill the goals defined by environmental authorities is an important aspect where plasma assisted combustion, PAC, might be an important tool. Plasma has the capability to stabilize flames under leaner conditions as well as extending the explosion limit [8]. Ju *et al* [8] have listed various areas where PAC has great potential, but also where there are major challenges in the future, for example, the lack of reliable kinetic models in the complex environments caused by the plasma.

Numerous investigations have been carried out to increase the knowledge of what conditions can be established with non-thermal plasmas. In a doctoral thesis by Jiajian Zhu several optical diagnostic techniques for various measurements in non-thermal plasmas are discussed [9]. For example, Rayleigh scattering may be used to measure gas temperatures in plasmas. Zhu *et al* [10] measured the translational temperature of the hot gas surrounding a plasma column using Rayleigh scattering from a frequency-doubled Nd:YAG laser and found that the translational temperature was roughly 1100 K. Reactive species, such as OH, H, O, and O_3, are important to measure since they can be utilized in various applications. For example, in plasma-based sterilization the germicidal effect is caused by O_3 and its interaction with cellular respiration [11] and in RF (radio-frequency) plasmas the fuel oxidation process is found to be triggered by O, H, and OH radicals [12]. For further details regarding various optical measurements of reactive species in atmospheric pressure non-thermal plasmas the reader is referred to the review article by Ono [13] and references therein. Also, Aldén *et al* [14] and Kohse-Höinghoaus [15] have reviewed different laser-based techniques to measure intermediate species relevant for combustion processes.

Imaging of radicals and species distributions using planar laser-induced fluorescence (PLIF) has shown great potential in a variety of research fields including plasma research. Various species can be imaged by forming the laser beam into a sheet and tuning the laser wavelength to match a molecular transition, e.g. OH [16, 17] at 283 nm and NO [18] at 226 nm.

Ozone has shown great potential for combustion enhancement since it thermally decomposes into O and O_2, initiating and accelerating chain-branching reactions, leading to both earlier CH_2O production and increasing the laminar flame speed [19, 20]. As already mentioned, ozone is one reactive species that is created in plasmas and several studies have been carried out to investigate ozone formation in plasmas using UV absorption. Two-dimensional (2D) UV absorption measurements in a streamer discharge have been undertaken by Hegeler *et al* [21], while Ono *et al* [22] conducted similar studies in a pulsed corona discharge as well as in a pulsed positive dielectric barrier discharge [23]. These authors have studied both the temporal and spatial distribution of ozone density by either mapping an area through pointwise measurements with a photomultiplier tube, PMT, or by expanding the beam and detecting the absorption with a CCD camera. Although 2D absorption measurements enhance the knowledge of plasma-produced ozone in the spatial domain, UV-absorption suffers from being a line-of-sight technique, for which data interpretation is ambiguous.

In the present work instantaneous 2D distributions of ozone, O_3, have been imaged in a gliding arc discharge by photofragmentation laser-induced fluorescence (PFLIF). A single laser pulse produced by a KrF excimer laser (248 nm) is used for photodissociation and resonant excitation. Within the pulse a photon first dissociates the O_3 molecule into an O atom and a vibrationally hot O_2 fragment, whereupon a second photon excites the O_2 fragment. The laser excited oxygen molecule then de-excites and emits fluorescence. For further details concerning PFLIF of ozone the reader is referred to [24]. Prior to the ozone measurements the lifetime of vibrationally hot O_2 was measured, both in a laminar ozone flow and in ozone produced by the gliding arc discharge, by letting a 266 nm laser pulse act as photolysis pulse. This arrangement allowed the 248 nm beam to probe the created hot O_2 fragments and the lifetime of hot O_2 could be extracted for both setups.

Experimental setup and measurement concept

The experiments were conducted in three different measurement configurations, case I, case II, and case III, see figure 1. In case I a pump–probe experiment was carried out in a laminar ozone flow. Here, a frequency quadrupled Nd:YAG laser (Quantel, Brilliant b) generated pulses of 266 nm radiation and acted as a photolysis laser. The laser was operating at a pulse repetition rate of 10 Hz with a pulse duration of roughly 5 ns. An injection-locked KrF excimer laser (Lambda Physik EMG 150 MSC), tunable from 247.9–248.9 nm, was used to probe the hot O_2 fragments. The laser was operated at a pulse repetition rate of 10 Hz, producing pulses of roughly 17 ns pulse duration and ~100 mJ pulse energy. The laser linewidth was ~0.2 cm^{-1} and tuned to an absorption peak, the P(13) line of the $O_2(B^3\Sigma_u^-, \nu' = 0 \leftarrow X^3\Sigma_g^-, \nu'' = 6)$ band, of the O_2 fragments. The two laser pulses, i.e. at 266 and 248 nm, were spatially overlapped prior to the measurement volume using a dichroic mirror, highly transmitting for the 266 beam and highly reflective for the 248 nm beam. The laser pulses were then guided through sheet-forming optics before propagating through the measurement volume, containing a well-defined O_3 flow before being terminated in a beam dump. The O_3 flow was generated by supplying oxygen through an ozone generator (O_3-Technology AC-20), and then issued into the probe volume through a Teflon pipe. The oxygen gas flow was controlled using mass flow controllers (Bronkhorst). The mass-flow rate of ozone could be varied either by varying the flow of oxygen or the efficiency of the ozone generator.

An intensified CCD camera, ICCD (Princeton Instruments, PIMAX III), was used to capture the O_2 emission. The ICCD camera was equipped with an 85 mm focal length UV lens and two long-pass filters, WG335 and a liquid n-butyl acetate filter, in front of the camera and thereby wavelengths longer than 320 nm were transmitted to the ICCD camera. A spectrograph (Shamrock 750i, Andor, 1200 grooves mm^{-1} grating) mounted with an ICCD camera (iStar, Andor) was employed in order to capture the emission spectra from excited O_2 fragments between 320 and 450 nm. The collection optics in front of the spectrograph consisted of two spherical lenses

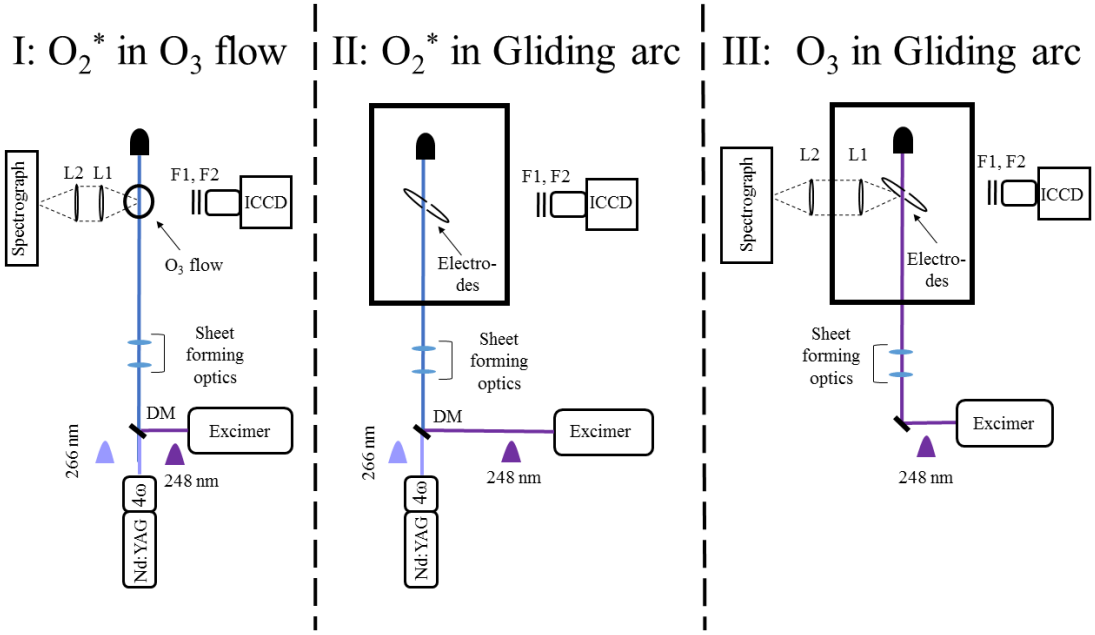

Figure 1. Schematic illustration of the three experimental setups. Abbreviation: F1 is a WG335 filter, F2 a liquid n-butyl acetate filter, DM a dichroic mirror, L1 and L2 are spherical lenses with focal lengths 200 and 300 mm, respectively.

with focal lengths, L2 = 300 mm and L1 = 200 mm, respectively. The fluence of the two laser beams in the probe volume were 0.03 J cm^{-2} for the 248 nm pulse and 0.1 J cm^{-2} for the 266 nm pulse. A pulse generator (BNC 575) provided pulses to synchronize the two lasers and also enabled variation of the time delay between the two laser beams. The measurement was carried out 3 cm above the output of the Teflon pipe providing the generated ozone flow.

In case II, the measurements were conducted in a gliding arc setup, see figure 1. Here, a plasma was created by the gliding arc discharge system, which was set in open air. It primarily consists of three components: electrodes, a power supply, and an air flow. The hollow tube-shaped electrodes are made of stainless steel, having an outer diameter of 3 mm and are internally water-cooled. The gliding arc discharge was driven by an AC power supply (Generator 6030, SOFTAL Electronic GmbH, Germany). For further details concerning the gliding arc discharge system the reader is referred to [17]. The pulse generator provided pulses to synchronize the two lasers with the plasma, and also enabled variation of the time delay between the two laser beams. The input power to the gliding arc was 1000 W and the air flow was kept at 15 l min^{-1}. Except for the ozone flow and the spectrograph in case I, the same equipment and laser fluences were used in case II. Finally, a third set of measurements were conducted, case III, where only the excimer laser was operating. This single-pulse configuration allowed the 248 nm laser pulse to act as both pump and probe pulse. A spectrograph was employed in order to capture the emission spectrum from excited O_2 fragments with the same configuration as in case I. Except for the lack of the 266 nm pulse, case III was operated with the same equipment and fluences as case II. For cases II and III the measurements were conducted 9 cm above the Teflon based plate which fixated the electrodes, see figure 2. In figure 2, the size and position of the 248 nm laser beam is shown as the horizontal blue line.

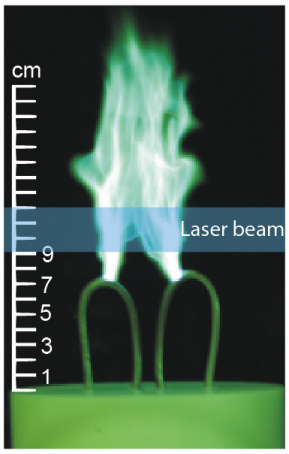

Figure 2. A photograph of an operating gliding arc discharge. The measurements were conducted 9 cm above the Teflon based plate which fixated the electrodes. The blue horizontal line shows the position of the 248 nm laser beam. The Teflon based plate is located below the ruler, the electrodes are positioned between 0 and 7 cm.

Results and discussion

Ozone was generated into the probe volume either by a laminar ozone flow or produced by the gliding arc discharge. For the lifetime measurements in cases II and III the gliding arc discharge was turned off prior to the arrival of the pump pulse to ensure that plasma-produced hot O_2 was negligible in the probe volume.

Pump-probe delay study in a laminar ozone flow

In plasmas both O_3 and hot O_2 are produced, wherefore an initial study was performed in order to measure the lifetime of hot O_2, see case I in figure 1. At ambient conditions O_3 has a lifetime of 30–40 min [19], whereas hot O_2 is expected to be short-lived before relaxing to a thermal equilibrium through

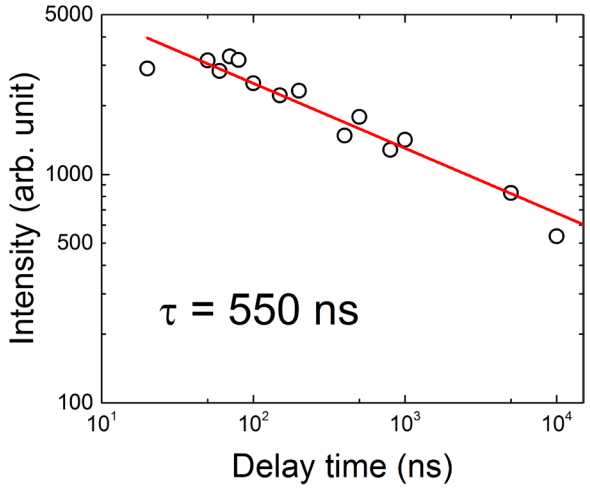

Figure 3. Pump-probe delay study of the O_2 fragment emission stemming from O_3 in a laminar ozone flow. In the logarithmic diagram the circular data points are from experiments, while the red line is a single exponential fit to the data points. The lifetime of hot O_2 is determined to be 550 ns.

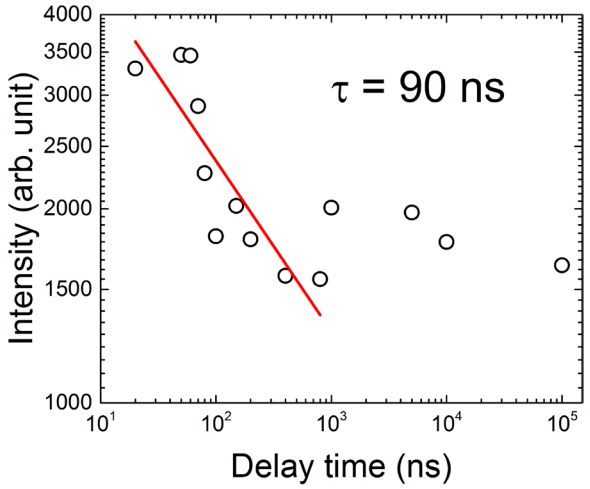

Figure 4. Pump-probe delay study of the O_2 fragment emission stemming from O_3 in the gliding arc discharge. The pump pulse was fired 0.5 ms after the high voltage was turned off and the measured lifetime of hot O_2 was 90 ns. The red line is a single exponential fit to the first part of the data points.

molecular collisions. Considering the different lifetimes of O_3 and hot O_2 at ambient conditions, an experiment was conducted to investigate the lifetime of hot O_2 in a laminar ozone flow. The photolysis of ozone and excitation of the O_2 fragments were therefore separated by two different laser pulses, 266 and 248 nm, respectively. Here, the 266 nm laser pulse acts as a pump-pulse and dissociates the ozone molecule into an oxygen atom and a vibrationally excited O_2 fragment, while the 248 nm laser pulse acts as a probe-pulse and excites the hot O_2 distribution to a higher electronic state. By varying the time delay between the pump and probe pulses, the lifetime of hot O_2 was determined. Figure 3 shows the detected O_2 fluorescence signal at different time delays of the probe pulse after dissociation of ozone. At $t = 0$ the pump pulse was fired and the ozone dissociated. Each measurement point is an average of 10 software (SW) accumulations each covering 50 hardware (HW) accumulations, which were performed in a gas flow containing roughly 4% ozone. A background image, where no lasers were fired, has been subtracted for all data points. The increase in signal during the first 100 ns is most probably a result of population of higher vibrational states than the O_2 $(X^3\Sigma_g^-, \nu'' = 6,7)$ after photolysis of ozone. The de-excitation of these states may lead to an initial increased population of the $\nu'' = 6{,}7$ states which results in an increase of the fluorescence signal. Similar results have been reported for $\nu'' = 8{,}9$ [25] upon 266 nm photolysis, in which vibrational population up to $\nu'' = 22$ is energetically possible. From this study a lifetime of 550 ns is obtained for vibrationally hot O_2 in the ozone flow. A spectroscopic investigation was conducted in order to verify that the detected signal was stemming from hot oxygen. It was found that the dispersed emission spectrum coincides with emission originating from vibrationally hot O_2 [24].

Pump-probe delay study in gliding arc

In a similar manner, as for the results presented in figure 3, the lifetime of hot O_2 was also investigated for ozone produced by the gliding arc discharge. The 266 nm laser pulse is used to dissociate ozone and the 248 nm laser pulse to probe the hot O_2 fragments at different time delays after dissociation, see case II in figure 1. The measurements were conducted 0.5 ms after the gliding arc discharge was turned off to ensure that the electron density was too low to produce hot O_2 [26]. The result is depicted in figure 4, where each measurement point is an average of 10 SW accumulations, each covering 50 HW accumulations. Each data point has been compensated for background recorded with no lasers fired. The input power to the gliding arc was 1000 W and the air flow was kept at 15 l min^{-1}. Due to the random fluctuations of the gliding arc discharge, the absolute value of the lifetime for the hot O_2 fluorescence signal is difficult to determine, but has a similar magnitude as the measurements performed in the ozone gas flow, 90 ns (±40 ns). From 20 to roughly 1000 ns there is a distinct signal drop, whereas for delay times longer than 1000 ns the signal is rather constant. This signal background is a result of self-photolysis from the 248 nm pulse, i.e. this signal is independent of the 266 nm pulse and the 248 nm pulse acts both as pump and probe pulse. The signal fluctuations are a result of the interaction between the turbulent gas flow and the transient gliding arc plasma. The location of the signal in the images recorded for each data point is essentially unchanged regardless of the time delay, indicating that the influence of the gas flow is minor. Potential signal interference from chemically and electronically produced hot O_2 is discussed below.

Lifetime of ozone produced by the gliding arc discharge

The lifetime of ozone generated by the gliding arc discharge was investigated for delay times between 0.5 and 5 ms after the discharge was turned off, i.e. case III in figure 1, and the result is shown in figure 5. For this study, only the 248 nm laser was operating, thus acting as both pump and probe laser. The discharge was turned off at $t = 0$ and the signal decay reveals the consumption of the plasma-produced ozone over

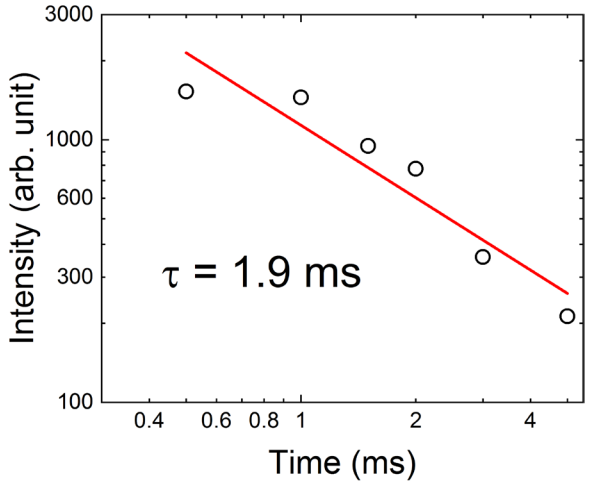

Figure 5. Lifetime of ozone produced by the gliding arc discharge. The gliding arc discharge has been turned off at $t = 0$ and the red line is a single exponential fit to the data points.

time. A signal lifetime of 1.9 ms is retrieved from the graph, where each measurement point is an average of 20 SW accumulations, each containing 50 HW accumulations. Each data point has been compensated for background recorded with the same settings but without firing any laser pulse. The influence of the gas flow on the data points is minor since the signal distribution in the images recorded for each data point is essentially unaffected by the time delay. A spectrograph was used to ensure that the detected emission was stemming from hot O_2. The ozone has a lifetime on the order of milliseconds, which compared to the lifetime of hot O_2 (~90 ns) is roughly four orders of magnitude longer. Thus, imaging of ozone using PFLIF with a 248 nm laser pulse is possible if the laser pulse is fired when the electron density is low enough to ensure that electron collisions will not put significant population in $\nu'' = 6,7$ of O_2. The electron density is, typically, low enough within tens of nanoseconds after turning off the high voltage [26]. Although, chemical reactions that produce hot O_2 will occur after the gliding arc has been shut off, the probability that these reactions will put significant populations in O_2 ($\nu'' = 6,7$) decreases rapidly after the discharge is shut off and after 0.5 ms the population is assumed to be negligibly small.

Electronically versus photochemically produced hot O_2

The one-pulse photofragmentation approach has a potential challenge in discriminating signal that stems from ozone and plasma-produced vibrationally excited oxygen ($\nu'' = 6,7$) in a plasma. Such vibrationally excited oxygen could potentially be a result of electronic collision excitation. Previously presented data indicate that the kinetic energy of the electrons and the ambient gas temperature in the gliding arc in the current study is around 0.8 eV and in the range of 1100–1600 K, respectively [10]. An oxygen molecule has to be in at least $\nu'' = 2$ to gain enough energy through an electronic collision to reach $\nu'' = 6$ [27]. At gas temperatures around 1100–1600 K, the fraction of O_2 that are in $\nu'' \geqslant 2$ is typically 1.5%–6% assuming a Boltzmann distribution. Under these conditions, typical cross section values for such electronic-collision excitations are on the order of 10^{-20} cm^2 (retrieved from extrapolation of table 5 in [28]). Given that the laser pulse duration was 17 ns, the pulse energy 40 mJ, $N_{O_3} = 1000$ ppm, $N_e = 7.3 \cdot 10^{18}$ m^{-3} [29], the number of hot O_2 ($\nu'' = 6,7$) that are created from electronic collisions, in this short time interval, was calculated to be roughly five orders of magnitude less than the hot O_2 ($\nu'' = 6,7$) fragments created by laser fragmentation of O_3. This large difference is a result of the hot O_2 being created from electronic collisions which is continuously produced over time by the gliding arc discharge, while all hot O_2 fragments produced by PFLIF of O_3 is created only during the 17 ns laser pulse duration. We therefore conclude that ozone imaging is possible when the gliding arc discharge is operating since any signal interference from hot O_2 produced by electronic collisions is negligible for this setup. It should, however, be emphasized that the signal interference from plasma-produced hot O_2 could vary for different plasma sources and must therefore be considered for the investigated plasma source to ensure accurate ozone visualization.

Imaging

The single-shot images shown in figure 6 display the 2D distribution of the O_2 fluorescence signal based on PFLIF of ozone, using 248 nm laser radiation, in the plasma produced by the gliding arc discharge, see case III. Here, figures 6(a) and (b) are images recorded when the discharge was on, while figure 6(c) is acquired 250 μs after the discharge was turned off. The air flow was kept at 15 l min^{-1} for all images, whereas the input power to the gliding arc was 600, 400, and 800 W for 6(a)–(c), respectively. A short camera gate, 50 ns, was kept for the result shown in figures 6(a) and (c), while the camera exposure time was long enough, 500 ns, for the data shown in figure 6(b) so that the plasma column could be clearly seen as the small string in the bottom center. The spatial resolution for all images in figure 6 is 0.043 mm/pixel. Furthermore, based on the aforementioned calculations it was concluded for this setup that the number density of naturally present vibrationally hot O_2 in the plasma was several orders of magnitude lower than the number density of vibrationally hot O_2 stemming from photolysis of O_3 and hence the plasma did not have to be turned off in order to measure O_3. The fluorescence from hot O_2 thus stems from O_3 whether the plasma is turned off or continuously running.

Figure 6(b) shows the spatial distribution of ozone in the vicinity of the discharge channel. Ozone has a distinct distribution characteristic compared with the distribution of OH, which has been reported in a previous work by Zhu *et al* [30]. They found a hollow structure for OH, which is not observed for O_3 in this work. Since ozone has a lifetime on the order of milliseconds, in the gliding arc setup, it is not surprising that O_3 is found in a region outside the plasma column, as can be seen in figure 6(b). The signal is wide compared to the plasma column, which also is a result of the long lifetime of ozone. In addition, the vibrationally excited O_2 molecules in $\nu'' = 6,7$ and electronically excited O_2 (in the $B^3\Sigma_u^-$ state) is unaffected by collisional

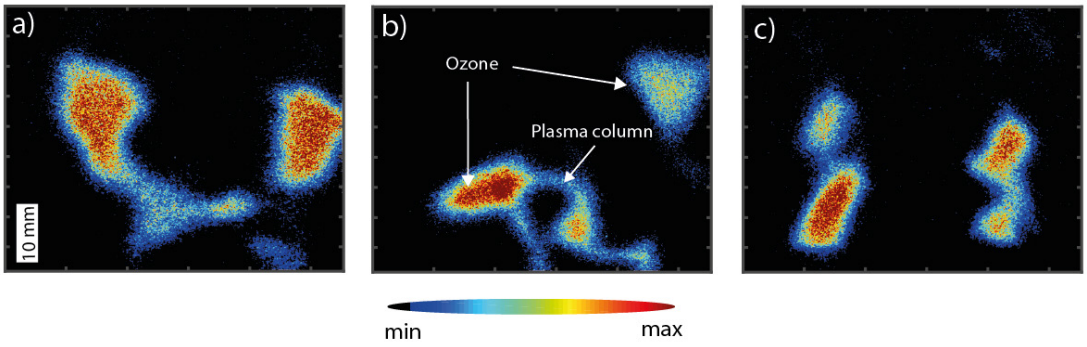

Figure 6. Imaging of ozone in the gliding arc discharge by PFLIF. Here, (a) and (b) were recorded when the discharge was on, while (c) was recorded 250 μs after the discharge was turned off.

quenching, since the vibrational energy transfer process is much slower than the laser pulse duration and predissociation is the dominating loss factor of the electronically excited state [24].

Summary and conclusion

In the presented study, a single laser beam from a KrF excimer laser was fired to visualize ozone in a gliding arc discharge. The concept is based on a pump-probe technique called PFLIF, where the 248 nm laser pulse acts both as pump and probe pulse. In this one-pulse configuration the pump pulse dissociates O_3 into O and vibrationally hot O_2 fragments, while the probe pulse excites the created hot O_2 fragment. Imaging of O_3 in the plasma must be carried out with caution since vibrationally hot O_2 can be produced by the plasma itself. The validity of applying this method to monitor ozone in a gliding arc was investigated by adding an additional 266 nm preceding laser pulse that acts as pump pulse, whereas the 248 nm pulse now mainly acts as a probe pulse. With this two-pulse configuration the lifetime of hot O_2 could be estimated both in a laminar O_3 flow and in the gliding arc discharge. It was found that the lifetime of hot O_2 is several orders of magnitude shorter than the lifetime of O_3 produced by the plasma, which ensures that O_3 can be monitored when the plasma is turned off. In addition, the amount of plasma-produced vibrationally hot O_2 was estimated to be several orders of magnitude lower than the amount of hot O_2 stemming from O_3, which enable ozone imaging with this method when the gliding arc plasma is present.

Acknowledgments

The authors would like to acknowledge the Swedish Research Council (VR), the Swedish Energy Agency (Energimyndigheten) through the Center for Combustion Science and Technology (CECOST), The European Research Council (through the advance grant TUCLA), and the Knut and Alice Wallenberg foundation for funding this project.

ORCID iDs

Kajsa Larsson https://orcid.org/0000-0002-6646-0486
Dina Hot https://orcid.org/0000-0003-4963-7849
Chengdong Kong https://orcid.org/0000-0003-3713-0653
Zhongshan Li https://orcid.org/0000-0002-0447-2748
Joakim Bood https://orcid.org/0000-0003-3339-9938
Andreas Ehn https://orcid.org/0000-0002-3716-8822

References

[1] Fridman A, Nester S, Kennedy L A, Saveliev A and Mutaf-Yardimci O 1999 Gliding arc gas discharge *Prog. Energy Combust. Sci.* **25** 211–31
[2] Lee D H, Kim K T, Cha M S and Song Y H 2007 Optimization scheme of a rotating gliding arc reactor for partial oxidation of methane *Proc. Combust. Inst.* **31** 3343–51
[3] Michael J B 2012 Localized Microwave Pulsed Plasmas for Ignition and Flame Front Enhancement *PhD Thesis* (Princeton, NJ: Princeton University Press)
[4] Rusterholtz D 2012 Nanosecond repetitively pulsed discharges in atmospheric pressure air *PhD Thesis* Ecole Centrale, Paris
[5] Fridman A, Gutsol A, Gangoli S, Ju Y and Ombrello T 2008 Characteristics of gliding arc and its application in combustion enhancement *J. Propuls. Power* **24** 1216–28
[6] Starikovskii A Y, Anikin N B, Kosarev I N, Mintoussov E I, Starikovskaia S M and Zhukov V P 2006 Plasma-assisted combustion *Pure Appl. Chem.* **78** 1265
[7] Ombrello T, Qin X, Ju Y, Gutsol A, Fridman A and Carter C 2006 Combustion enhancement via stabilized piecewise nonequilibrium gliding arc plasma discharge *AIAA J.* **44** 142–50
[8] Ju Y and Sun W 2015 Plasma assisted combustion: progress, challenges, and opportunities *Combust. Flame* **162** 529–32
[9] Zhu J 2015 Optical diagnostics of non-thermal plasmas and plasma-assisted combustion *PhD Thesis*
[10] Zhu J *et al* 2017 Translational, rotational, vibrational and electron temperatures of a gliding arc discharge *Opt. Express* **25** 3343–51
[11] Laroussi M 2005 Low temperature plasma-based sterilization: overview and state-of-the-art *Plasma Process. Polym.* **2** 391–400
[12] Starikovskaia S M 2006 Plasma assisted ignition and combustion *J. Phys. D: Appl. Phys.* **39** R265–99
[13] Ono R 2016 Optical diagnostics of reactive species in atmospheric-pressure nonthermal plasma *J. Phys. D: Appl. Phys.* **49** 83001
[14] Aldén M, Bood J, Li Z and Richter M 2011 Visualization and understanding of combustion processes using spatially and temporally resolved laser diagnostic techniques *Proc. Combust. Inst.* **33** 69–97
[15] Kohse-Höinghaus K 1994 Laser techniques for the quantitative detection of reactive intermediates in combustion systems *Prog. Energy Combust. Sci.* **20** 203–79

[16] Sankaranarayanan R, Pashaie B and Dhali S K 2000 Laser-induced fluorescence of OH radicals in a dielectric barrier discharge *Appl. Phys. Lett.* **77** 2970–2

[17] Sun Z W *et al* 2013 Optical diagnostics of a gliding arc *Opt. Express* **21** 6028–44

[18] Kanazawa S *et al* 2005 Wide-range two-dimensional imaging of NO density profiles by LIF technique in a corona radical shower reactor *IEEE Trans. Ind. Appl.* **41** 200–5

[19] Weng W *et al* 2015 Investigation of formaldehyde enhancement by ozone addition in CH_4/air premixed flames *Combust. Flame* **162** 1284–93

[20] Ehn A *et al* 2015 Plasma assisted combustion: effects of O_3 on large scale turbulent combustion studied with laser diagnostics and large eddy simulations *Proc. Combust. Inst.* **35** 3487–95

[21] Hegeler F and Akiyama H 1997 Spatial and temporal distributions of ozone after a wire-to-plate streamer discharge *IEEE Trans. Plasma Sci.* **25** 1158–65

[22] Ono R and Oda T 2004 Spatial distribution of ozone density in pulsed corona discharges observed by two-dimensional laser absorption method *J. Phys. D: Appl. Phys.* **37** 730–5

[23] Ono R and Oda T 2007 Ozone production process in pulsed positive dielectric barrier discharge *J. Phys. D: Appl. Phys.* **40** 176–82

[24] Larsson K *et al* 2017 Quantitative imaging of ozone vapor using photofragmentation laser-induced fluorescence (LIF) *Appl. Spectrosc.* **71** 1578–85

[25] Yamasaki K, Fujii H, Watanabe S, Hatano T and Tokue I 2006 Efficient vibrational relaxation of $O_2(X^3\Sigma_g^-, \nu = 8)$ by collisions with CF_4 *Phys. Chem. Chem. Phys.* **8** 1936–41

[26] Dogariu A, Shneider M N and Miles R B 2013 Versatile radar measurement of the electron loss rate in air *Appl. Phys. Lett.* **103** 224102

[27] Allan M 1995 Measurement of absolute differential cross sections for vibrational excitation of O_2 by electron impact *J. Phys. B: At. Mol. Opt. Phys.* **28** 5163–75

[28] Itikawa Y 2009 Cross sections for electron collisions with oxygen molecules *J. Phys. Chem. Ref. Data* **38** 1–20

[29] Zhu J *et al* 2014 Sustained diffusive alternating current gliding arc discharge in atmospheric pressure air *Appl. Phys. Lett.* **105** 2012–7

[30] Zhu J *et al* 2014 Dynamics, OH distributions and UV emission of a gliding arc at various flow-rates investigated by optical measurements *J. Phys. D: Appl. Phys.* **47** 295203